NANO LETTERS

Letter

Cite This: *Nano Lett.* 2020, 20, 546−552

pubs.acs.org/NanoLett

Metal/LiF/Li_2O Nanocomposite for Battery Cathode Prelithiation: Trade-off between Capacity and Stability

Junmou Du,[†] Wenyu Wang,[†] Alex Yong Sheng Eng,[‡] Xiaoxiao Liu,[†] Mintao Wan,[†] Zhi Wei Seh,[‡] and Yongming Sun*,[†]

[†]Wuhan National Laboratory for Optoelectronics, Huazhong University of Science and Technology, Wuhan 430074, China

[‡]Institute of Materials Research and Engineering, Agency for Science, Technology and Research (A*STAR), 2 Fusionopolis Way, Innovis, Singapore 138634, Singapore

Supporting Information

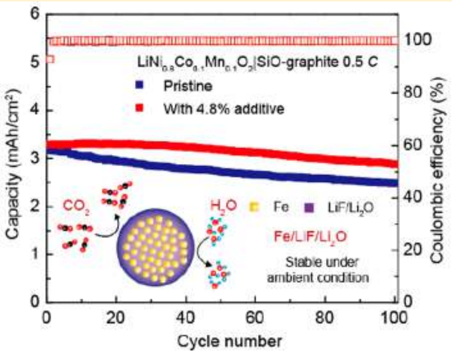

ABSTRACT: Lithium-ion batteries (LIBs) are currently dominating the portable electronics market and supplying power for electric vehicles and grid-level storage. However, lithium loss in the formation cycle at the anode side reduces the energy density of state-of-the-art LIBs with carbon anode materials. This situation will be even more severe for future LIBs using high-capacity Si-based anode materials. In this study, a transition metal-based nanocomposite with built-in lithium source was synthesized, featuring Fe nanodomains with a size of ~5 nm uniformly dispersed in a hybrid Li_2O and LiF matrix with intimate contact between them. The Fe/LiF/Li_2O nanocomposite released a high Li-ion capacity of 550 mA h/g based on a multielectron inverse conversion reaction during the first-cycle charge process and exhibited better ambient stability than the counterpart with a pure Li_2O matrix and also a lower lithium-extraction voltage and faster reaction kinetics than the counterpart with a pure LiF matrix. Serving as an additive to various cathodes (e.g., $LiCoO_2$, $LiFePO_4$, and $LiNi_{1-x-y}Co_xMn_yO_2$), the Fe/LiF/Li_2O nanocomposite showed excellent lithium compensation effect. Using 4.8 wt % Fe/LiF/Li_2O additive based on the total mass of the electrodes, a $LiNi_{0.8}Co_{0.1}Mn_{0.1}O_2$|SiO-graphite full cell with a high cathode mass loading of 20 mg/cm^2 exhibited a high reversible capacity of 2.9 mA h/cm^2 at 0.5 C after 100 cycles which is a 15% increase in comparison to the counterpart without the prelithiation additive. After the Fe/LiF/Li_2O nanocomposite was immersed into the electrolyte and rested for 72 h, the content of iron metal in the electrolyte was negligible, indicating that this prelithiation additive was stable in the electrolyte and would not cause any side reactions, such as the shuttle of iron ions during cycling. The high "donor" Li-ion capacity, good ambient stability, and its compatibility with existing cathode materials and battery fabrication processes make the Fe/LiF/Li_2O nanocomposite a promising cathode prelithiation additive to offset the initial lithium loss and improve the energy density of LIBs.

KEYWORDS: *Fe/LiF/Li_2O nanocomposite, cathode prelithiation, initial lithium loss, stability, lithium-ion batteries*

Lithium-ion batteries (LIBs) have dominated the market of portable electronics and are extending their applications to electric vehicles and grid-level energy storage.[1−5] However, conventional LIBs with a carbon anode and a transition metal oxide cathode cannot meet the fast increasing demand of energy density for various applications. Until now, much attention has been paid to the development of new high-capacity battery materials (e.g., sulfur cathode, O_2 cathode, Si anode, and Li metal anode).[6−12] Although there is still a long time for the success of these new battery chemistries, the effect of improving current battery systems is more achievable in the near future. In conventional LIBs, lithium ions stored in the cathode transfer to the anode in the initial charging process, accompanied by the formation of a solid electrolyte interphase (SEI) on the anode surface.[13,14] This process irreversibly consumes part of active lithium and reduces the capacity and energy density of batteries. Prelithiation can introduce extra active lithium into battery systems and is highly promising in compensating for the initial lithium loss and also increasing the energy density of LIBs.

Various prelithiation approaches have been explored to date, including electrochemical prelithiation, chemical prelithiation, and using prelithiation additives for electrodes.[15−17] The prelithiation additives can be added to the negative or positive electrode and thus are potentially compatible with the industrial battery fabrication technology.[18,19] Some representative anode prelithiation materials, such as stabilized lithium metal powders,[20,21] lithium silicide nanoparticles,[22] and $Li_{2.6}Co_{0.4}N$,[23] exhibit high "donor" Li-ion specific capacity and are promising in eliminating the initial active lithium loss in LIBs. However, these anode prelithiation materials show high chemical reactivity with the existing polar solvents [e.g.,

Received: October 16, 2019
Revised: November 26, 2019
Published: November 27, 2019

DOI: 10.1021/acs.nanolett.9b04278
Nano Lett. 2020, 20, 546−552

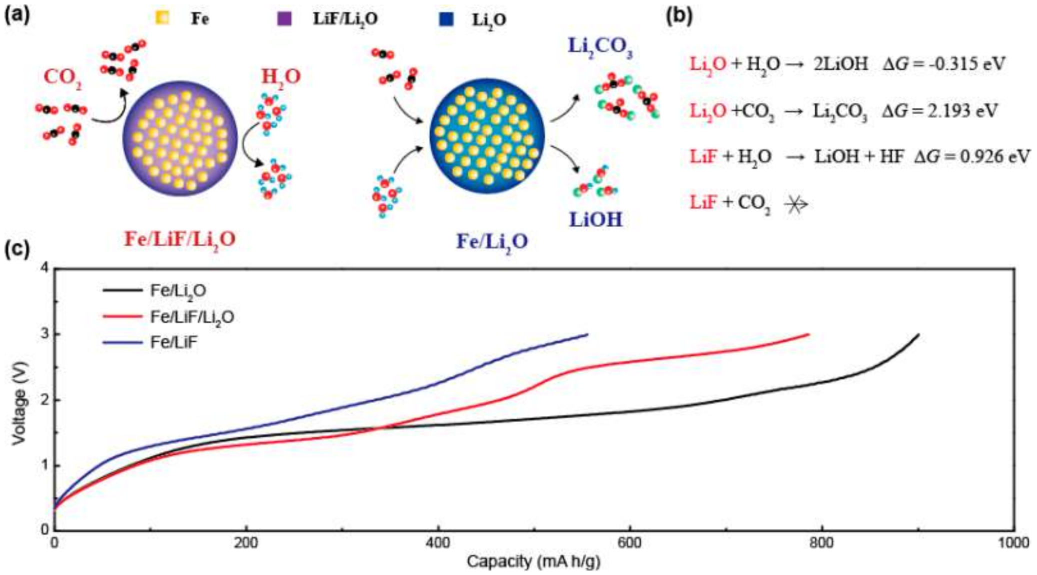

Figure 1. (a) Comparison of the chemical stability between Fe/LiF/Li_2O and Fe/Li_2O nanocomposites in the ambient air. (b) Calculated reaction Gibbs free energy of Li_2O and LiF reacting with H_2O and CO_2 by thermodynamic method. (c) Typical charge curves of Fe/LiF, Fe/LiF/Li_2O, and Fe/Li_2O nanocomposites prepared using electrochemical lithiation using Fe_2O_3, FeOF, and FeF_3.

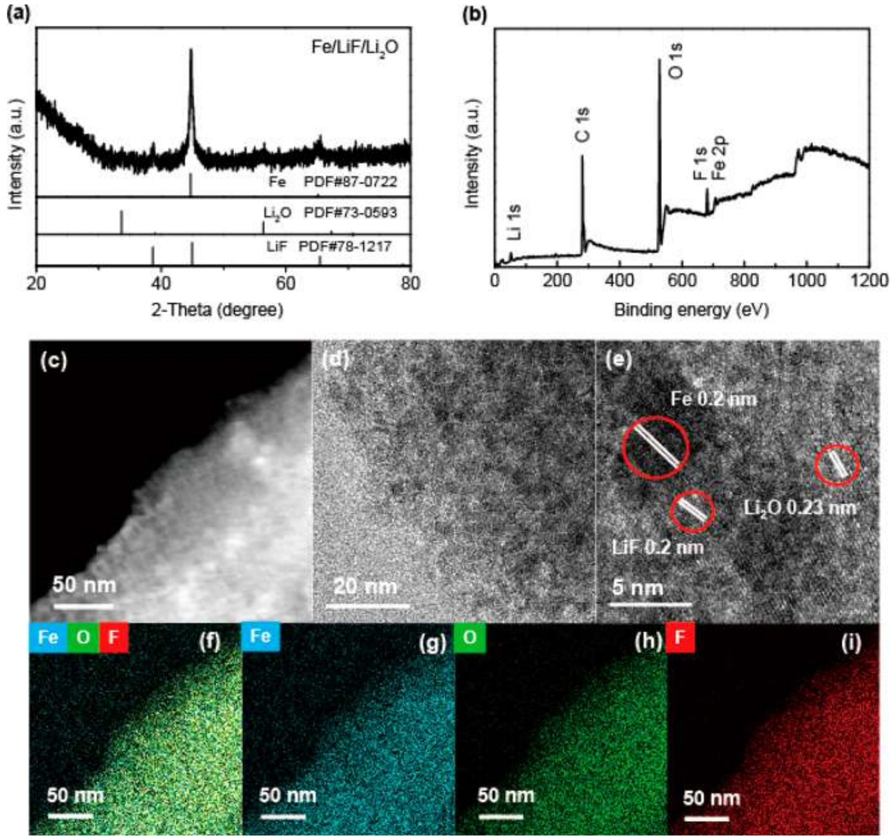

Figure 2. XRD pattern of (a) Fe/LiF/Li_2O. (b) XPS profile of as prepared Fe/LiF/Li_2O nanocomposites. (c) STEM image of Fe/LiF/Li_2O. (d,e) HRTEM images of Fe/LiF/Li_2O. (f−i) Elemental EDX maps of Fe/LiF/Li_2O.

N-methyl-2-pyrrolidone (NMP) and water] for battery slurry preparation and are not stable in ambient conditions, which seriously impede their real applications in battery industry.

Compared to anode prelithiation materials, cathode prelithiation materials exhibit higher open circuit voltage (e.g., >1 V) and better stability in ambient atmosphere. Moreover, some cathode prelithiation additives often have much better compatibility with NMP, the mostly widely used solvent in cathode slurry preparation, making them practical in the battery industry.[24,25] Lithium rich materials, such as Li_2NiO_2[26,27] and Li_6CoO_4,[28] have been widely investigated as cathode prelithiation additives. However, their application is restricted by their low capacities (300−400 mA h/g). Sacrificial lithium salts, including $Li_2C_4O_4$, LiC_2O_2, $Li_2C_3O_5$,

DOI: 10.1021/acs.nanolett.9b04278
Nano Lett. 2020, 20, 546−552

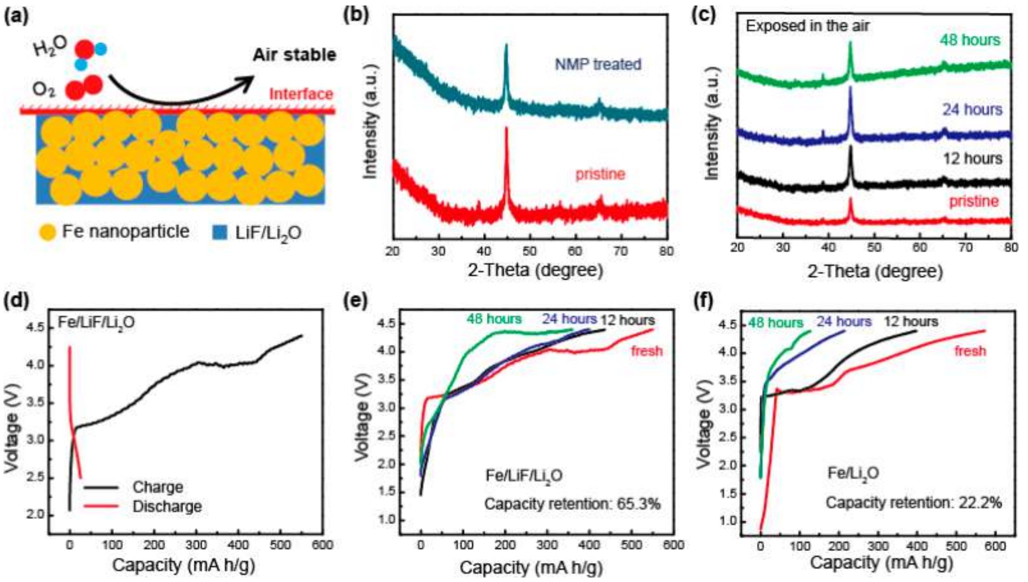

Figure 3. (a) Schematic illustration of Fe/LiF/Li_2O nanocomposite exposed to the ambient air. XRD patterns of Fe/LiF/Li_2O nanocomposites after NMP-solvent treatment (b) and storage in the ambient atmosphere (20% humidity) (c) for different time. (d) Initial charge−discharge curves of Fe/LiF/Li_2O at a current density of 25 mA/g. Initial charge curve of (e) the Fe/LiF/Li_2O and (f) Fe/Li_2O nanocomposite after storage in the ambient atmosphere (20% humidity) for different times. The current density is 25 mA/g.

and $Li_2C_4O_6$,[29] deliver relatively higher specific capacities (300−600 mA h/g). However, undesired gases would be produced, accompanied by their decomposition.[30−33] In our previous work, conversion reaction-based prelithiation reagents including M (M = Fe, Co, or Ni)/Li_2O, M/LiF, and M/Li_2S composite have been explored and these additives can release high Li-ion capacities (e.g., >500 mA h/g) without gas products during the Li-ion extraction process.[34,35] However, Li_2S is highly toxic and reactive with trace H_2O in the ambient air, which makes M/Li_2S composite impractical for industrial application. With better stability than Li_2S, Li_2O is still hygroscopic and it easily reacts with humidity in the ambient air to form LiOH (ΔG = −0.315 eV, Figure 1a,b). The formation of LiOH reduces the "donor" Li-ion capacity of M/Li_2O composite and its alkalinity may easily lead to the failure of slurry preparation. In contrast, LiF is an ambient-stable compound. The calculated Gibbs free energy change of LiF reactions with H_2O and CO_2 indicate that LiF has much better resistance to H_2O and CO_2 than Li_2O (Figure 1a,b). Thus, M/LiF composites are stable in ambient conditions and compatible with the existing positive electrode fabrication process. However, due to the low electronic conductivity of MF_x and high ionicity of M−F bonding,[36] the conversion reactions of MF_x have slow kinetics and high reaction voltage, which may lead to low practical "donor" Li-ion capacities of M/LiF composites in the charge cutoff voltage of current oxide and phosphate cathodes (<4.3 V vs Li^+/Li). On the other hand, high Li-ion capacity can be easily extracted from M/Li_2O composite in the charge cutoff voltage of the widely used cathodes due to the low ionicity of M−O bonding and relatively higher electronic conductivity of MO_x (Figure 1c).[36]

In this work, to achieve good stability and high "donor" Li-ion capacities of conversion reaction-based prelithiation materials, a Fe/LiF/Li_2O nanocomposite with built-in Li_2O and LiF has been prepared. Fe, Li_2O, and LiF nanodomains with the size of ∼5 nm were uniformly dispersed in the composite and contacted with each other closely. The introduction of both LiF and Li_2O could make a trade-off between the stability and "donor" lithium-ion capacity. As expected, the Fe/LiF/Li_2O nanocomposite exhibited a high specific capacity of 550 mA h/g in the initial charge process. Importantly, such prelithiation additive showed good compatibility with existing battery fabrication process. The Fe/LiF/Li_2O nanocomposite was successfully applied to various cathodes, including $LiCoO_2$, $LiFePO_4$, and $LiNi_{0.6}Co_{0.2}Mn_{0.2}O_2$. Impressively, 15% increase in reversible capacity was achieved for a $LiNi_{0.8}Co_{0.1}Mn_{0.1}O_2$|SiO-graphite full cell with high cathode mass loading (20 mg/cm^2) using 4.8 wt % such additive.

Results and Discussions. The Fe/LiF/Li_2O nanocomposites were synthesized through the reaction between the as-prepared FeOF powder (Figures S1 and S2) and molten metallic lithium in an argon atmosphere. During the synthesis, FeOF gradually reacted with molten lithium to produce the Fe/LiF/Li_2O nanocomposite ($FeOF + 3Li \rightarrow Li_2O + LiF + Fe$) under stirring (Figure S3). After the reaction, a black powder was achieved. As shown in Figure 2a, the XRD diffraction peaks of the product were ascribed to Fe (JCPDS 87-0722), Li_2O (JCPDS 73-0593), and LiF (JCPDS 78-1217), respectively. None of the characteristic peaks of FeOF were observed, indicating that FeOF was completely transformed to Fe, Li_2O, and LiF. The low intensity and significant broadening of these peaks indicated the low crystallinity and small crystallite size of the Fe, Li_2O, and LiF nanoparticles. SEM results showed the irregular secondary particles of the Fe/LiF/Li_2O nanocomposite with particle size ranged from 1 to 10 μm (Figure S4). The large particle size of the nanocomposite leads to a low accessible surface area to the ambient environment, which is beneficial for improving the ambient stability. Information about the composition and the surface electronic state of the as-achieved Fe/LiF/Li_2O composite were obtained by XPS measurement (Figure 2b and Figure S5). Signals of Fe, O, F, and Li elements were observed in the survey XPS spectrum of the product, suggesting the existence of these elements in the nanocomposite. The high-resolution Fe 2p XPS spectrum revealed a doublet at 709.7 eV for Fe $2p_{3/2}$ and

DOI: 10.1021/acs.nanolett.9b04278
Nano Lett. 2020, 20, 546−552

723.2 eV for Fe $2p_{1/2}$ due to the partial surface oxidation of iron nanoparticles.[37,38] Li 1s peak was located at 55.1 eV in the high-resolution Li 1s spectrum and F 1s peak was centered at 684.5 eV in the high-resolution F 1s spectrum, indicating the existence of LiF. An O 1s peak was observed at 531.3 eV, which mainly arose from Li_2O. These results verified the existence of Fe, Li_2O, and LiF in the nanocomposite. TEM and STEM images were performed to further investigate the microstructure of the as-achieved Fe/LiF/Li_2O nanocomposite (Figure 2c–i). Clear dark/light contrast was observed in the STEM image due to the difference of atomic mass (Figure 2c). Bright dots with the size of ~5 nm were uniformly dispersed in the observed area of the nanocomposite, which arose from the heavy Fe element, corresponding to Fe nanoparticles. The dark area in the STEM corresponded to the Li_2O and LiF. Intimate contact between the Fe, LiF, and Li_2O nanoparticles was verified. The uniform composite structure was also shown under TEM (Figure 2d). HRTEM result further provided detailed information on the components in the nanocomposite. Clear lattice fringes with spacings of 0.2 nm, 0.2 nm, and 0.23 nm were observed, which were ascribed to Fe (110), LiF (200), and Li_2O (200), respectively. The average size of the Fe nanoparticles embedded in LiF/Li_2O matrix was ~5 nm (Figure 2e and Figure S6). The ultrafine particle size of the LiF, Li_2O, and Fe and their close contact are beneficial for improving the Li-extraction kinetics during the electrochemical charging process and providing high lithium-ion capacity. Furthermore, the EDX elemental mapping revealed that the elements of Fe, Li, F, and O were evenly dispersed, suggesting the uniform structure of Fe/LiF/Li_2O nanocomposite again.

To investigate the compatibility of Fe/LiF/Li_2O nanocomposite with industrial cathode processing using a polar NMP solvent, the Fe/LiF/Li_2O nanocomposite was dispersed in NMP and rested for 10 min. The composition and phase information were investigated after the treatment. The XRD pattern showed same peak positions and similar intensity for the as-treated Fe/LiF/Li_2O nanocomposite in comparison to the fresh sample (Figure 3b), suggesting the good stability of the Fe/LiF/Li_2O in the polar NMP solvent. On the other hand, to measure the ambient stability, the as-prepared Fe/LiF/Li_2O nanocomposite was rested in air with 20% humidity for different time (12, 24, and 48 h), which was much higher than the value in dry rooms for industrial electrode fabrication. Even after 48 h, the Fe/LiF/Li_2O nanocomposite remained stable according to the XRD result, indicating slow reaction with humidity under the test condition (Figure 3c). Due to the good compatibility with the NMP solvent and stability in ambient condition, the as-prepared Fe/LiF/Li_2O nanocomposite is potentially compatible with the current positive electrode fabrication process.

For the application of the Fe/LiF/Li_2O nanocomposite as a prelithiation reagent in battery industry, it is necessary to measure the stability of the Fe contained within the Fe/LiF/Li_2O nanocomposite in the liquid electrolyte. This is because the dissolution of Fe in the electrolyte would result in low Coulombic efficiency, capacity decay of LIBs and even safety concerns.[39] To investigate the dissolubility of the Fe of the nanocomposite in electrolytes, Fe/LiF/Li_2O composite powder was dispersed in a widely used commercial carbonate-based electrolyte. After 72 h, the electrolyte filtrate was collected and evaporated. The residue was dissolved by nitric acid for the measurement of inductively coupled plasma mass spectrometry (ICP-MS). The result in Table S1 showed that the Fe ions in the sample and the control were both at the low ppb level with similar values, indicating the good chemical stability of the Fe/LiF/Li_2O nanocomposite in the carbonate electrolyte.

To investigate the "donor" Li-ion capacity of the Fe/LiF/Li_2O nanocomposite, the Fe/LiF/Li_2O electrode was successfully prepared using the regular positive electrode fabrication process. The galvanostatic charge/discharge measurement of the Fe/LiF/Li_2O electrode was performed with the charge cutoff voltage of 4.4 V and discharge cutoff voltage of 2.5 V (Figure 3d). Two voltage slopes were observed during the charging process due to the complex lithium extraction reactions of the Fe/LiF/Li_2O electrode. The first voltage slope started from 3.1 V with the capacity contribution of 260 mA h/g. This voltage slope mainly arose from the inverse conversion reaction of Fe/Li_2O because of the faster reaction kinetics between Fe and Li_2O. The second voltage slope was located between 3.8–4.1 V, which was mainly contributed by the conversion reaction from Fe/LiF to FeF_3. The product after delithiation was investigated using TEM. Uniform nanoparticles with lattice fringes corresponding to Fe_2O_3 and FeF_3 were observed (Figure S7). Moreover, the existence of Fe_2O_3 and FeF_3 in the delithiated product was also confirmed by XPS measurement (Figure S8). These results indicated the inverse conversion reaction mechanism ($3Fe + 3LiF + 3Li_2O \rightarrow Fe_2O_3 + FeF_3 + 9Li^+ + 9e^-$) for the Fe/LiF/$Li_2O$ product during the delithiation process. The extracted Li-ion capacity reached 550 mA h/g during the first-cycle charge process with the cutoff voltage of 4.4 V. Because of the large voltage hysteresis of the conversion reaction, the lithiation voltage of the as-achieved prelithiated material was much lower than the cutoff voltage of the existing cathodes (Figure S9). With a cutoff voltage of 2.5 V, the electrode exhibited a low discharge capacity of 23 mA h/g (Figure 3d). Thus, the "donor" Li-ion capacity of the Fe/LiF/Li_2O prelithiation material was as high as 527 mA h/g. These results indicate that the as-achieved Fe/LiF/Li_2O nanocomposite is not relithiated before the cutoff discharge voltage of the cathodes and thus functions only as a high-efficiency prelithiation additive material within the voltage window to compensate for the initial lithium loss in LIBs. As a comparison, a LiF/Li_2O mixture only showed a specific charge capacity of 6 mA h/g (Figure S10), which is due to the high decomposition voltage of LiF and Li_2O. This investigation indicated the importance of the introduction of a transition metal which changed the lithium-extraction reaction mechanism and lowered the lithium-extraction voltage. Moreover, the overall size of the Fe/LiF/Li_2O nanocomposite was slightly reduced after delithiation (Figure S11). Although the shrinkage of the particles is inevitable for Fe/LiF/Li_2O, it does not cause the obvious thickness/volume change of the cathode due to its small amount (usually <5%) and the porous electrode structure which can buffer the volume change. The electrode fabrication process of Fe/LiF/Li_2O nanocomposite was carried out here with a regular slurry processing using NMP solvent and PVDF binder, compatible with the current battery fabrication process. Thus, the Fe/LiF/Li_2O nanocomposite can be directly introduced to cathodes during their fabrication. We further investigated the effect of ambient exposure on the capacity of the Fe/LiF/Li_2O electrode. The results showed that the charge capacity of the Fe/LiF/Li_2O electrode faded slowly with the increase of time exposed to ambient air due to the slow deliquescence of Li_2O in the air. A capacity of 359 mA h/g was achieved after storage in ambient condition for 48 h

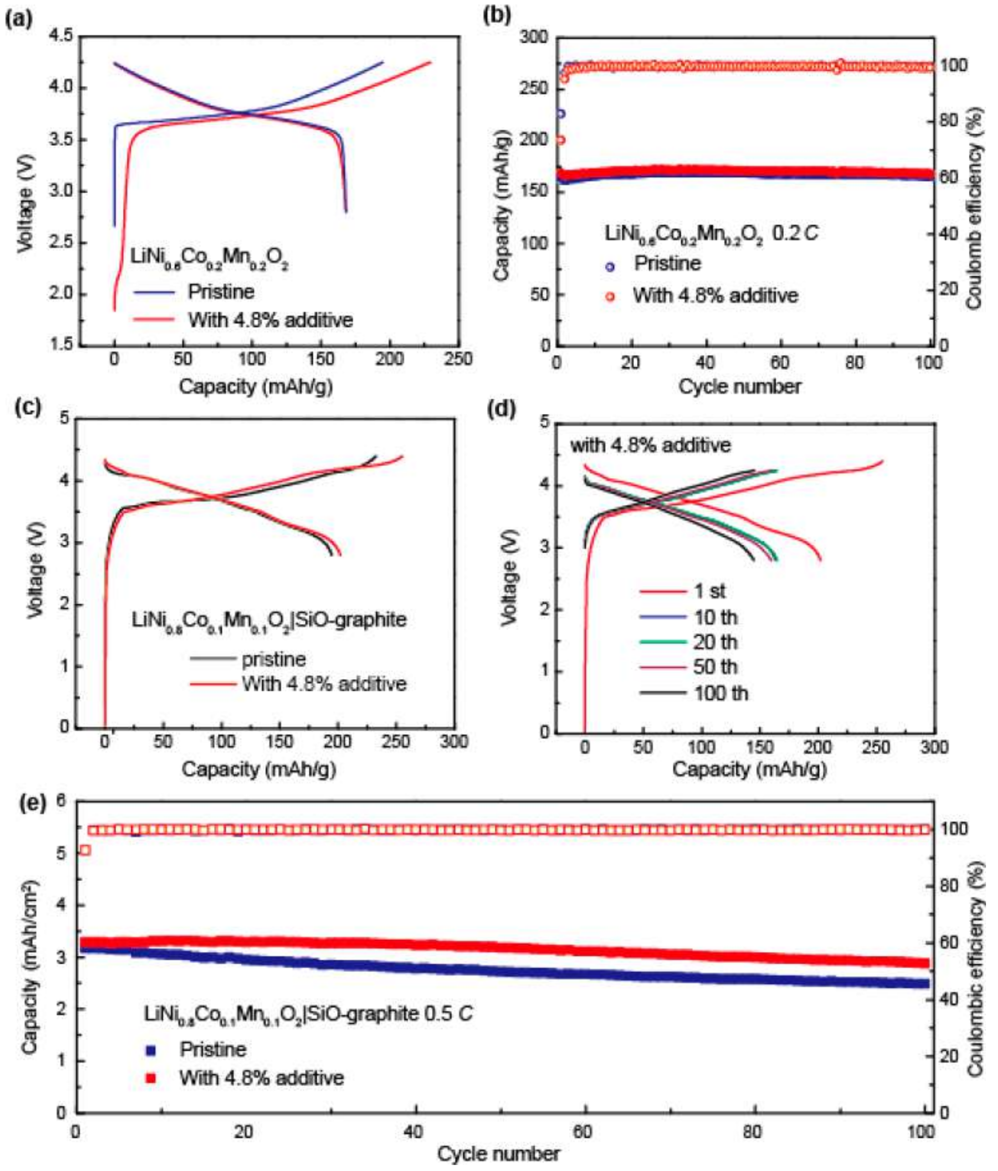

Figure 4. (a,b) Initial charge−discharge curves and cycling stability of $LiNi_{0.6}Co_{0.2}Mn_{0.2}O_2$ half cells with and without Fe/LiF/Li_2O additive. (c−e) Initial charge−discharge curves and cycling stability of $LiNi_{0.8}Co_{0.1}Mn_{0.1}O_2$|SiO-graphite full cells with and without Fe/LiF/Li_2O additive. The initial charge/discharge current density is 0.1 C.

which is 65% of the initial value (Figure 3e). As a comparison, the Fe/Li_2O nanocomposite was fabricated through the reaction between Fe_2O_3 and molten lithium. The Fe/Li_2O electrode maintained only 22% of its initial capacity (127 mA h/g) after 48 h storage in ambient condition (Figure 3f) due to the high reaction activity of Li_2O to moisture in the air. The enhanced ambient stability of the Fe/LiF/Li_2O nanocomposite arises from the dense structure of the micrometer-scale secondary particles which suppresses the penetration of O_2 and H_2O into the particles (Figure S4, Figure 2) and ambient stable LiF which helps to inhibit the attack of H_2O and O_2.

The lithium compensation effect of the Fe/LiF/Li_2O nanocomposite for various cathodes was further carried out. The Fe/LiF/Li_2O nanocomposite was introduced into $LiNi_{0.6}Co_{0.2}Mn_{0.2}O_2$, $LiCoO_2$, and $LiFePO_4$ electrodes using a regular slurry casting method. Figure 4a shows the initial charge curves of $LiNi_{0.6}Co_{0.2}Mn_{0.2}O_2$ electrode with and without the Fe/LiF/Li_2O additive. The $LiNi_{0.6}Co_{0.2}Mn_{0.2}O_2$ electrode with 4.8% Fe/LiF/Li_2O additive showed slightly lower open-circuit voltage (OCV) than the pristine electrode. During the charge process, the $LiNi_{0.6}Co_{0.2}Mn_{0.2}O_2$ electrode with 4.8% Fe/LiF/Li_2O additive exhibited an extended voltage slope between 2.0−4.25 V in comparison to the pristine $LiNi_{0.6}Co_{0.2}Mn_{0.2}O_2$ electrode due to the extraction of lithium ions from the Fe/LiF/Li_2O nanocomposite. The first-cycle charge capacity of the $LiNi_{0.6}Co_{0.2}Mn_{0.2}O_2$ electrode with 4.8% additive was 229 mA h/g, which was 31 mA h/g (15.6%) higher than the pristine $LiNi_{0.6}Co_{0.2}Mn_{0.2}O_2$ electrode. This result indicated that the active lithium in the Fe/LiF/Li_2O nanocomposite was successfully extracted during the first-cycle charge process. The extracted Li-ion specific capacity from the Fe/LiF/Li_2O additive was as high as 486 mA h/g. Importantly, the addition of Fe/LiF/Li_2O nanocomposite did not cause any negative effect on the discharge process. The capacity−voltage plots for the $LiNi_{0.6}Co_{0.2}Mn_{0.2}O_2$ electrodes with and without the additive overlapped well and released the same discharge capacity (168 mA h/g). Therefore, a high prelithiation efficiency can be achieved by using the Fe/LiF/Li_2O cathode prelithiation reagent. After 100 charge/discharge cycles, 99.1% capacity retention was achieved for the $LiNi_{0.6}Co_{0.2}Mn_{0.2}O_2$ electrode with the addition of Fe/LiF/Li_2O, which is similar to the counterpart without the additive (Figure 4b and Table S2). This result indicated that the Fe/LiF/Li_2O had good chemical stability and compatibility to the $LiNi_{0.6}Co_{0.2}Mn_{0.2}O_2$ electrode and did not cause any negative effect on the cycling stability of the cathode. To show the generality of using the Fe/LiF/Li_2O prelithiation reagent to various cathodes, we investigated the $LiCoO_2$ and $LiFePO_4$ cathodes with 4.8% Fe/LiF/Li_2O additive, respectively. The first charge capacities of $LiCoO_2$ and $LiFePO_4$ electrodes were 181 and 162 mA h/g, respectively. With 4.8 wt % Fe/LiF/Li_2O additive, their first-cycle charge capacities increased to 215 mA h/g for the $LiCoO_2$ electrode and 191 mA h/g for the $LiFePO_4$ electrode, which were 34 mA h/g (18.8%) and 29 mA h/g (17.9%) higher than their counterparts, respectively (Figure S12). On the basis of the mass of the Fe/LiF/Li_2O additive in the electrodes, the extracted Li-ion capacities were 532 mA h/g and 470 mA h/g, respectively. All the cathodes with the Fe/LiF/Li_2O additive showed similar reversible discharge capacities to the pristine cathodes and stable cycling after the first cycle (Figures S12 and S13), indicating the generality for using Fe/LiF/Li_2O as an effective prelithiation additive. It is noted that the initial discharge capacities of all the measured cathodes remain unchanged although their initial charge capacity increase with the Fe/LiF/Li_2O additive. Therefore, the calculated initial Coulombic efficiency of the cathode with the Fe/LiF/Li_2O additive is reduced in comparison to the pristine electrode. To verify the effect of the Fe/LiF/Li_2O additive on improving the capacity and energy density of full cells, full batteries ($LiNi_{0.8}Co_{0.1}Mn_{0.1}O_2$|SiO−graphite) without and with 4.8 wt % Fe/LiF/Li_2O additive was fabricated and their electrochemical performance was evaluated. Initial charge−discharge curves of the full batteries are shown in Figure 4c. The $LiNi_{0.8}Co_{0.1}Mn_{0.1}O_2$ electrode with the Fe/LiF/Li_2O additive delivered an initial charge capacity of 5.1 mA h/cm^2 (255 mA h/g) and an initial discharge capacity of 4.1 mA h/cm^2 (204 mA h/g) at 0.1 C, which was 0.3 mA h/cm^2 (23 mA h/g) and 0.1 mA h/cm^2 (10 mA h/g) higher than the pristine counterpart, respectively. Figure 4d,e showed the cycling stability of the full batteries, and the full battery with Fe/LiF/Li_2O additive exhibited better capacity retention (88.4%) than the counterpart without the additive (78.8%). The electrode with the Fe/LiF/Li_2O additive released 2.9 mA h/cm^2 or 144.7 mA h/g after 100 cycles at 0.5 C, a 15% increase in comparison to the pristine counterpart based on the weight of the active material and additive (Table S2 and Figure S14). Additionally, the capacity of the full battery after prelithiation was slightly improved at various current densities in comparison to the counterpart without prelithiation (Figure S15). To further investigate the electrochemical kinetics of the full battery, cyclic voltammetry (CV) and electrochemical impedance spectroscopy (EIS) were carried out. The CVs of the full battery with and without Fe/LiF/Li_2O showed similar redox peaks in the voltage range of 3−4.4 V (Figure S16), indicating the addition of Fe/LiF/Li_2O did not change the electrochemical reaction. The electrical conductivity of the full battery was evaluated by EIS (Figure S17). It showed that the full batteries with and without prelithiation reagent had similar impedance after cycling, suggesting that Fe/LiF/Li_2O had limited effect on the impedance of the full battery. Therefore, the Fe/LiF/Li_2O nanocomposite is a promising prelithiation additive for various cathodes to compensate for the initial lithium loss in industrial applications due to their high prelithiation efficiency and compatibility with existing commercial cathode materials and battery fabrication process.

In conclusion, a stable Fe/LiF/Li_2O nanocomposite was successfully designed and synthesized for cathode prelithiation to compensate for the initial lithium loss and to improve the energy density of batteries. The Fe/LiF/Li_2O nanocomposite was composed of micrometer-size secondary particles built by Fe, Li_2O, and LiF nanoparticles with uniform dispersion and intimate interaction. Regular electrode fabrication processing can be used to prepare the Fe/LiF/Li_2O electrode or cathodes with the Fe/LiF/Li_2O additive using a slurry coating method and NMP solvent. Electrochemical measurement showed that the Fe/LiF/Li_2O nanocomposites exhibited high "donor" lithium-ion capacity of 523 mA h/g, three times that of the existing cathodes through an inverse conversion reaction ($3Fe + 3LiF + 3Li_2O \rightarrow Fe_2O_3 + FeF_3 + 9Li^+ + 9e^-$) during the initial charge/discharge process. With 4.8 wt % Fe/LiF/Li_2O additive, $LiCoO_2$, $LiFePO_4$, and $LiNi_{0.6}Co_{0.2}Mn_{0.2}O_2$ electrodes showed 16−20% increase in specific capacity during the initial charge process, in comparison to the pristine cathodes. A high reversible capacity of 2.9 mA h/cm^2 was achieved after 100 cycles for a $LiNi_{0.8}Co_{0.1}Mn_{0.1}O_2$|SiO−graphite full cell with 4.8 wt % cathode prelithiation additive after 100 charge/discharge cycles at 0.5 C at a high cathode mass loading of 20 mg/cm^2, which was 15% higher than the pristine counterpart. The good ambient stability of the Fe/LiF/Li_2O nanocomposite was confirmed by the ambient atmosphere (20% humidity) resting experiment, exhibiting good ambient stability. Moreover, iron ions were not detected in the electrolyte after soaking with the Fe/LiF/Li_2O nanocomposite for a set time, indicating that the Fe nanoparticles in the nanocomposite were stable in the electrolyte. These results indicate high prelithiation efficiency, good compatibility with existing battery electrode fabrication methods, and good chemical stability of the Fe/LiF/Li_2O nanocomposites. This work opens the prospect of developing new and promising cathode prelithiation additives for practical application in the battery industry today.

■ ASSOCIATED CONTENT

Ⓢ Supporting Information

The Supporting Information is available free of charge at https://pubs.acs.org/doi/10.1021/acs.nanolett.9b04278.

Experimental details and additional characterizations (PDF)

■ AUTHOR INFORMATION

Corresponding Author

*E-mail: yongmingsun@hust.edu.cn.

ORCID

Zhi Wei Seh: 0000-0003-0953-567X
Yongming Sun: 0000-0001-8528-525X

Notes

The authors declare no competing financial interest.

■ ACKNOWLEDGMENTS

This work was supported by the Natural Science Foundation of China (Grant 51802105) and Innovation Fund of Wuhan National Laboratory for Optoelectronics. The authors would like to thank the Analytical and Testing Center of Huazhong University of Science and Technology as well as the Center for Nanoscale Characterization and Devices of Wuhan National Laboratory for Optoelectronics for providing the facilities to conduct the characterization. Z.W.S. acknowledges the support of the Singapore National Research Foundation (NRF-NRFF2017-04).

REFERENCES

(1) Chan, C. K.; Peng, H. L.; Liu, G.; Mcllwrath, K.; Zhang, X. F.; Huggins, R. A.; Cui, Y. *Nat. Nanotechnol.* **2008**, *3*, 31−35.

(2) Armand, M.; Tarascon, J.-M. *Nature* **2008**, *451*, 652−657.

(3) Goodenough, J. B.; Kim, Y. *Chem. Mater.* **2010**, *22*, 587−603.

(4) Scrosati, B.; Hassoun, J.; Sun, Y.-K. *Energy Environ. Sci.* **2011**, *4*, 3287.

(5) Tarascon, J.-M.; Armand, M. *Nature* **2001**, *414*, 359−367.

(6) Peng, Z. Q.; Freunberger, S. A.; Chen, Y. H.; Bruce, P. G. *Science* **2012**, *337*, 563−566.

(7) Ji, X. L.; Lee, K. T.; Nazar, L. F. *Nat. Mater.* **2009**, *8*, 500−506.

(8) Wu, H.; Cui, Y. *Nano Today* **2012**, *7*, 414−429.

(9) Xu, W.; Wang, J. L.; Ding, F.; Chen, X. L.; Nasybulin, E.; Zhang, Y. H.; Zhang, J. G. *Energy Environ. Sci.* **2014**, *7*, 513−537.

(10) Seh, Z. W.; Sun, Y. M.; Zhang, Q.; Cui, Y. *Chem. Soc. Rev.* **2016**, *45*, 5605−5634.

(11) Li, Y.; Wang, W.; Liu, X.; Mao, E.; Wang, M.; Li, G.; Fu, L.; Li, Z.; Eng, A. Y. S.; Seh, Z. W.; Sun, Y. *Energy Storage Mater.* **2019**, *23*, 261.

(12) Sun, Y. M.; Seh, Z. W.; Li, W. Y.; Yao, H. B.; Zheng, G. Y.; Cui, Y. *Nano Energy* **2015**, *11*, 579−586.

(13) Verma, P.; Maire, P.; Novák, P. *Electrochim. Acta* **2010**, *55*, 6332−6341.

(14) Xu, K. *Chem. Rev.* **2004**, *104*, 4303−4417.

(15) Mai, L.; Xu, L.; Hu, B.; Gu, Y. *J. Mater. Res.* **2010**, *25*, 1413−1420.

(16) Aravindan, V.; Lee, Y.-S.; Madhavi, S. *Adv. Energy Mater.* **2017**, *7*, 1602607.

(17) Holtstiege, F.; Baermann, P.; Noelle, R.; Winter, M.; Placke, T. *Batteries* **2018**, *4*, 4.

(18) Llave, E. d. l.; Borgel, V.; Park, K. J.; Hwang, J. Y.; Sun, Y. K.; Hartmann, P.; Chesneau, F. F.; Aurbach, D. *ACS Appl. Mater. Interfaces* **2016**, *8*, 1867−1875.

(19) Kim, H. J.; Choi, S.; Lee, S. J.; Seo, M. W.; Lee, J. G.; Deniz, E.; Lee, Y. J.; Kim, E. K.; Choi, J. W. *Nano Lett.* **2016**, *16*, 282−288.

(20) Jarvis, C. R.; Lain, M. J.; Gao, Y.; Yakovleva, M. *J. Power Sources* **2005**, *146*, 331−334.

(21) Li, Y.; Fitch, B. *Electrochem. Commun.* **2011**, *13*, 664−667.

(22) Zhao, J.; Lu, Z.; Liu, N.; Lee, H. W.; McDowell, M. T.; Cui, Y. *Nat. Commun.* **2014**, *5*, 5088.

(23) Shodai, T.; Sakurai, Y.; Suzuki, T. *Solid State Ionics* **1999**, *122*, 85−93.

(24) Sun, Y.; Lee, H.-W.; Zheng, G.; Seh, Z. W.; Sun, J.; Li, Y.; Cui, Y. *Nano Lett.* **2016**, *16*, 1497−1501.

(25) Sun, Y. M.; Lee, H. W.; Seh, Z. W.; Liu, N.; Sun, J.; Li, Y. Z.; Cui, Y. *Nat. Energy* **2016**, *1*, 1−7.

(26) Kim, M. G.; Cho, J. *J. Mater. Chem.* **2008**, *18*, 5880.

(27) Park, H.; Yoon, T.; Kim, Y.-U.; Ryu, J. H.; Oh, S. M. *Electrochim. Acta* **2013**, *108*, 591−595.

(28) Su, X.; Lin, C. K.; Wang, X. P.; Maroni, V. A.; Ren, Y.; Johnson, C. S.; Lu, W. Q. *J. Power Sources* **2016**, *324*, 150−157.

(29) Shanmukaraj, D.; Grugeon, S.; Laruelle, S.; Douglade, G.; Tarascon, J.-M.; Armand, M. *Electrochem. Commun.* **2010**, *12*, 1344−1347.

(30) Park, K.; Yu, B. C.; Goodenough, J. B. *Adv. Energy Mater.* **2016**, *6*, 1502534.

(31) Sun, Y. M.; Li, Y. B.; Sun, J.; Li, Y. Z.; Pei, A.; Cui, Y. *Energy Storage Mater.* **2017**, *6*, 119−124.

(32) Abouimrane, A.; Cui, Y. J.; Chen, Z. H.; Belharouak, I.; Yahia, H. B.; Wu, H. M.; Assary, R.; Curtiss, L. A.; Amine, K. *Nano Energy* **2016**, *27*, 196−201.

(33) Zhan, Y. J.; Yu, H. L.; Ben, L. B.; Chen, Y. Y.; Huang, X. J. *Electrochim. Acta* **2017**, *255*, 212−219.

(34) Li, H.; Richter, G.; Maier, J. *Adv. Mater.* **2003**, *15*, 736−739.

(35) Poizot, P.; Laruelle, S.; Grugeon, S.; Dupont, L.; Tarascon, J. M. *Nature* **2000**, *407*, 496−499.

(36) Li, C.; Chen, K.; Zhou, X.; Maier, J. *npj Comput. Mater.* **2018**, *4*, 4.

(37) Schubert, J. S.; Popovic, J.; Haselmann, G. M.; Nandan, S. P.; Wang, J.; Giesriegl, A.; Cherevan, A. S.; Eder, D. *J. Mater. Chem. A* **2019**, *7*, 18568−18579.

(38) Xu, X. J.; Yang, Y.; Jia, Y. F.; Lian, X. Y.; Zhang, Y.; Feng, F.; Liu, Q. L.; Xi, B. D.; Jiang, Y. H. *Chem. Eng. J.* **2019**, *374*, 776−786.

(39) Zhan, C.; Wu, T.; Lu, J.; Amine, K. *Energy Environ. Sci.* **2018**, *11*, 243−257.

DOI: 10.1021/acs.nanolett.9b04278
Nano Lett. 2020, 20, 546−552